Electronic Response of Assemblies of Designer Atoms: The Metal−Insulator Transition and the Role of Disorder

F. Remacle[†] and R. D. Levine[‡]

Contribution from the Département de Chimie, B6, Université de Liège, B 4000 Liège, Belgium, The Fritz Haber Research Center for Molecular Dynamics, The Hebrew University, Jerusalem 91904, Israel, and Department of Chemistry and Biochemistry, University of California−Los Angeles, Los Angeles, California 90095

Received May 10, 1999

Abstract: Quantum dots present the chemist with the opportunity to synthesize atomic-like building blocks with made-to-measure electronic properties. For the theorists this allows a study of the same Hamiltonian for a range of parameters. Here we consider a lattice of quantum dots, where the dots can be prepared with a narrow distribution of properties but are never quite identical. This is unlike an ordered lattice of atoms or molecules. We report computations of the frequency-dependent dielectric response of a two-dimensional array of quantum dots, as a function of the distance between the dots. When the dots are not closely packed, the response is dominated by the Coulomb repulsion of electrons (of opposite spin) on a given dot. This gives rise to an insulator−metal transition as the expanded array is compressed. The interplay between the three effects, the "disorder" due to the size, shape, and environmental fluctuations of the dots, the coupling of adjacent dots, and the Coulomb repulsion are studied as functions of the lattice spacing. The computations are performed in the approximation where each dot carries one valence electron, but these electrons are fully correlated so as to fully account for the Coulomb blocking. This is possible by a diagonalization of the Hamiltonian in a many-electron basis. Comparison is made with experimental results for the dielectric response, as described in a companion to this paper.

1. Introduction

The ability to synthesize quantum dots of different materials and of variable sizes[1−4] allows us to consider what the electronic structure of assemblies of such dots will be like. Besides the fact that the properties of the components of the assembly can be selected, the coupling between the dots can be tuned. This can be achieved in discrete steps, by changing the ligands that passivate the dots—more on this point below—and also continuously by a compression of a lattice of dots.[5−7] However, the dots are never quite identical in size nor are the organic ligands needed to protect them packed in an identical way. The role of this local disorder can be studied in a simple approximation where each dot is mimicked as an atom with one valence orbital.[8] Due to their proximity the sites are coupled. When this coupling is strong enough it can bridge the (possibly, small) differences in the excitation energies of two neighboring sites. This allows for facile electron transfer from one dot to another, resulting in the formation of a band of delocalized states, as in a metal. When the coupling is weak, the excitation remains localized and the lattice behaves as an insulator. That disorder can cause such a transition between the two regimes is known in solid state theory, where it is named after Anderson.[9−11] Here, however, the array is finite in size.

The coupling of adjacent dots is due to the overlap of their wave functions. Part of the fascination of monolayers of quantum dots is that this coupling strength can be tuned by compressing the lattice.[6] Since the overlap is expected to depend exponentially on the inter-dot distance, the range of tuning is considerable. Here we refine our earlier work by allowing for the Coulomb repulsion between the electrons, an effect which is also present in molecules,[12] and which is important at large separations between the dots. The valence orbital on the atom can be empty, or it can accommodate one or two electrons (of different spins; the Pauli exclusion principle keeps electrons of the same spin effectively apart). When there is a second electron in the valence orbital there will be a Coulombic repulsion between these two electrons. This repulsion can be measured by scanning tunneling microscopy[13] (STM). In other words, due

* Corresponding author. Fax: 972-2-6513742. E-mail: rafi@fh.huji.ac.il.
[†] Université de Liège. Chercheur Qualifié, FNRS, Belgium.
[‡] The Hebrew University and University of California−Los Angeles.

(1) Bawendi, M. G.; Steigerwald, M. L.; Brus, L. E. *Annu. Rev. Phys. Chem.* **1990**, *41*, 477−96.
(2) Murray, C. B.; Kagan, C. R.; Bawendi, M. G. *Science* **1995**, *270*, 1335−1338.
(3) Alivisatos, A. P. *Science* **1996**, *271*, 933−937.
(4) Chen, S.; Ingram, R. S.; Hostetler, M. J.; Pietron, J. J.; Murray, R. W.; Schaaff, T. G.; Khoury, J. T.; Alvarez, M. M.; Whetten, R. L. *Science* **1998**, *280*, 2098−2101.
(5) Collier, C. P.; Vossmeyer, T.; Heath, J. R. *Annu. Rev. Phys. Chem.* **1998**, *49*, 371−404.
(6) Markovich, G.; Collier, C. P.; Henrichs, S. E.; Remacle, F.; Levine, R. D.; Heath, J. R. *Acc. Chem. Res.* **1999**, *32*, 415−423.
(7) Collier, C. P.; Saykally, R. J.; Shiang, J. J.; Henrichs, S. E.; Heath, J. R. *Science* **1997**, *277*, 1978−1981.
(8) Remacle, F.; Collier, C. P.; Heath, J. R.; Levine, R. D. *Chem. Phys. Lett.* **1998**, *291*, 453−458.
(9) Anderson, P. W. *Concepts in Solids*; Benjamin: Palo Alto, CA, 1971.
(10) Imada, M.; Fujimori, A.; Tokura, Y. *Rev. Mod. Phys.* **1998**, *70*, 1039−1263.
(11) Zallen, R. *The Physics of Amorphous Solids*; Wiley: New York, 1983.
(12) Parr, R. G. *Quantum Theory of Molecular Electronic Structure*; Benjamin: New York, 1963.
(13) Medeiros-Ribeiro, C.; Ohlberg, D. A. A.; Williams, R. S.; Heath, J. R. *Phys. Rev. B* **1999**, *59*, 1633−1636.

10.1021/ja9915448 CCC: $19.00
Published on Web 04/04/2000

to its finite size, a dot has a finite capacity for accommodating extra electrons. This hinders conductivity, and if the capacitance is small enough the material will act as an insulator. The importance of this (the so-called Mott[14] mechanism, also known as "Coulomb blocking") can be judged from the limit when the dots are far apart and very weakly coupled.[10,14] The lowest energy states have one electron per site. There is no first-order change in energy of these states because the inter-dot coupling, requiring an electron transfer, has no diagonal elements. The change in energy due to the coupling is then given by second-order perturbation theory as (coupling)^2/(charging energy). As the dots are compressed, this effective coupling increases until it can bridge the variations in the excitation energy of adjacent dots. The computations below include the effects of charging energy. The charging energy will be smaller for larger dots and, in general, will be significantly smaller than that for atoms in ordinary molecules.

In the terminology of quantum chemistry, allowing explicitly for the repulsion between electrons requires refining the electronic Hamiltonian from a Hückel to, for example, a Pariser−Parr−Pople (PPP) Hamiltonian.[12] The PPP Hamiltonian includes electron repulsion also for electrons on different sites. A simpler version, known as the Hubbard model,[15] incorporates only the repulsion between electrons (of opposite spins) on the same site.

The linear[16] and nonlinear[7] frequency responses of a hexagonal planar array of organically functionalized Ag quantum dots have been measured as functions of the inter-dot separation.[6] Additional discussion and results are presented in the preceding paper[17] and elsewhere.[5,18] The experimental results exhibit a qualitative change in the electronic response when the lattice is compressed. We here discuss these changes as manifestations of the Mott and Anderson transitions. The physical picture and detailed computations, as discussed below, are that the Mott transition occurs for a somewhat wider lattice spacing, while the Anderson transition occurs upon further compression. The limiting behavior of a Mott insulator or an (Anderson) conductor are distinct because both experiment[7] and computations[8] suggest that the coupling between the dots falls exponentially with their separation. Intermediate between the two there can be a regime where the coupling between the dots is strong enough to be comparable to the charging energy yet not strong enough to bridge the variations in the site energies. This intermediate regime is possible because of the relatively low charging energy of the dots. In this regime, charge can migrate from a dot to its near neighbors, but overall, the charge is still localized.

The conclusions of this paper depend on the magnitude and range of the interaction between adjacent dots. We therefore emphasize that this interaction is determined from fitting the previously measured nonlinear optical response,[8,19] and these values have not been readjusted. Also, the charging energy is taken as the value measured in the STM experiment.[13]

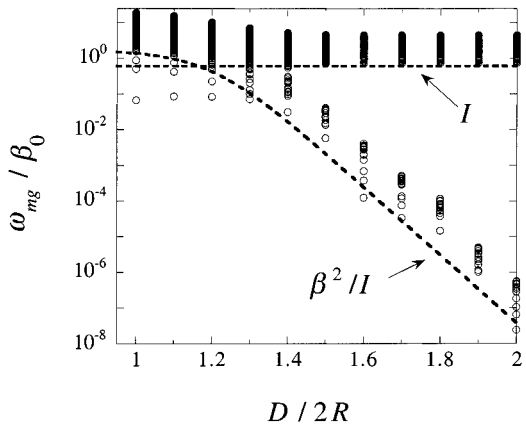

Figure 1. The 783 transition frequencies, determined by diagonalizing the full Hamiltonian of a hexagonal array of seven dots, plotted vs the compression parameter $D/2R$. D is the distance between the centers of the dots whose mean radius is R. These transition frequencies, from the ground to all 783 excited states, are one input needed for computing the dielectric constant. The other input is the dipole strengths of these transitions, which is shown in Figure 3. Figure 1 also shows (dashed curves) two excitation energies measured with respect to the ground state of the noninteraction dots. I is the charging energy, the energy needed to transfer an electron to an already occupied site. All states with excitation energies above I will have some ionic character. β is the strength of coupling of the near neighboring dots. When β is small, β^2/I is the energy shift of the states that have exactly one electron per dot, see text. The Mott insulator−metal transition occurs when the dot−dot coupling can overcome the charging energy. The simple argument says that this is when $\beta = I$. The detailed computations, as shown, indicate that this occurs at a somewhat higher value of $D/2R$. The exponential decline of β with $D/2R$, eq 2.3, has been previously determined[8] by comparison to the results of the measurement[7] of the second harmonic optical response. This gives a range parameter $1/L = 5.5$, which justifies the assumption that only near neighboring dots are directly coupled.

The range of the interaction between adjacent dots that we use is consistent with our theoretical estimate[19] based on through-space charge transfer. Since this range plays such a critical role, it will clearly be of interest to synthesize dots where the ligands will facilitate a through-bond charge transfer.

The experimental results are given as a function of the lattice parameter $D/2R$, where D is the distance between the centers of two adjacent dots and R is the radius of the dot. The present and earlier[8,19] results show that the Anderson transition to a delocalized electronic phase occurs at $D/2R < 1.4$. The "disorder" required for an Anderson transition is due to the inevitable, albeit narrow, size distribution of the dots, the possible deviations of a dot from spherical packing, and fluctuations in the organic ligands of the dot. We here report that the computed electronic response also exhibits a Mott transition at $D/2R > 1.3$ (Figure 1).

The computation of the electronic response is fully quantum mechanical. The dielectric function is computed from the eigenstates of the Hamiltonian. The role of the Coulomb repulsion is taken explicitly into account rather than by a self-consistent field approximation. Even for a tiny array, and keeping only one electronic state per dot, the number of many-electron states of the array that need to be included in the full basis is large (784 states for the minimal hexagonal array of seven dots; the next completed hexagonal array has 19 sites, and this corresponds to 2 821 056 160 states). The diagonalization is made practical by using a matrix representation of the Hamiltonian in a basis of spin and (anti)symmetry-adapted many-electron zero-order states that belong to an irreducible

(14) Mott, N. F. *Metal−Insulator Transitions*; Taylor & Francis: London, 1990.
(15) Hubbard, J. *Proc. R. Soc.* **1963**, *276*, 238−257.
(16) Markovich, G.; Collier, C. P.; Heath, J. *Phys. Rev. Lett.* **1998**, *80*, 3807−3810.
(17) Henrichs, S.; Collier, C. P.; Saykally, R. J.; Shen, Y. R.; Heath, J. R. *J. Am. Chem. Soc.* **2000**, *122*, 4077−4083 (preceding paper in this issue).
(18) Collier, C. P. Ph.D. Thesis, University of California, Berkeley, CA, 1998.
(19) Remacle, F.; Collier, C. P.; Markovich, G.; Heath, J. R.; Banin, U.; Levine, R. D. *J. Phys. Chem. B* **1998**, *102*, 7727−7734.

representation of the unitary group $U(n)$. These spin-adapted many-electron states correspond to the Gelfand−Tsetlin basis set for the irreducible representation.[20,21]

The dissipation effect that is included in all the present computations is a finite damping width of the excited electronic states. In some computations we also include a possible scrambling of the phase of the electron that is transferred between adjacent dots. Such a phase randomization will modify the electronic conduction from a coherent one to a hopping mechanism. Elsewhere we will discuss activated hopping in more detail. For the present we note only that the thermally induced hopping contribution is most likely at the lowest frequencies. The comparison of the present computations with the experimental results for the low-frequency ($\omega \rightarrow 0$) limit, while acceptable, is therefore not necessarily physically meaningful. The results for this regime are accordingly not shown, but they are available from the authors upon request.

Computing the response function requires not only the eigen energies of the system but also the dipole matrix elements. To do so we do *not* make the common π electron theory approximation that the states of adjacent sites are orthogonal. Rather, we do allow for overlap, and this makes the transition dipole matrix elements a sensitive function of the distance between the sites. It is this dependence of the dipole matrix element on the lattice parameter that makes the response function such a sensitive probe of the nature of the wave function.

This paper begins with a discussion of the Hamiltonian (section 2). At the suggestion of the editor and the referees, the discussion puts special emphasis on the more chemical context. The technical aspects of generating the basis used to obtain the Hamiltonian matrix are given elsewhere.[22] Section 3 presents the formalism for computing the dielectric constant and the complex modulus. The results are presented in section 4.

2. A Hamiltonian for Designer Atoms

In the simplest approximation one can regard each quantum dot as an atom carrying one valence electron and otherwise neglect the internal structure of the dots. [Note: Quantum dots have quite low-lying single electron excited states. For smaller dots, these are higher than the mean thermal energy. If need be, these can be taken into account using the extended Hückel Hamiltonian,[23] which allows more than one orbital per site.] This serves to center attention on those properties of the dots that are readily amenable to experimental control. Specifically, these properties will appear directly as parameters of the Hamiltonian. This approach is similar to the neglect of the electronic core of atoms in π electron theories.[12] The electronic Hamiltonian is then a Hückel (tight binding)−Hubbard Hamiltonian where each site carries one orbital. The Hubbard modification is the explicit inclusion of electronic correlation as a term that takes into account the repulsion of electrons of opposite spin when they are on the same site. As we discuss below, the role of the charging energy will be taken fully into account and not treated as an approximation (such as via a mean field in which each electron moves). The PPP Hamiltonian[12] takes into account also the electron repulsion for electrons on different sites. It can be used without an increase in our computational effort. We chose not to do so because unlike for the charging energy itself, estimating the additional repulsion terms is not trivial, and we did not want a computation with parameters which cannot be independently determined. The quantum dots are arranged in a two-dimensional hexagonal lattice geometry where the distance between the dots, D, is measured in terms of the mean diameter of the individual dots, $2R$.

The Hamiltonian for an array of n sites is written as

$$H = \sum_{i=1}^{n} \alpha_i \hat{E}_{ii} + \sum_{\substack{i=1 \\ \text{near neighbors}}}^{n} \beta_{ij} \hat{E}_{ij} + \frac{1}{2} \sum_{i=1}^{n} I_i \hat{E}_{ii} (\hat{E}_{ii} - 1) \quad (2.1)$$

The first two terms in (2.1) are from the usual Hückel Hamiltonian, where α_i is the ionization potential (IP) of the dot and the coupling, β_{ij}, is the transfer integral, which is nonzero between near neighbors only. $\hat{E}_{ii}$ is the operator which determines the charge on the site i, while $\hat{E}_{ij}$ moves an electron from site j to site i.

The dots are prepared by wet chemical methods, and the size distributions that are currently achieved are narrow enough for them to assemble into a lattice. However, the individual dots are not identical, and the α_i's fluctuate within a range $\alpha_0 \pm (\Delta\alpha/2) \equiv \alpha_0(1 \pm (\delta\alpha/2))$ due to variation in the sizes, irregularity with respect to the spherical shape, and variations in the ligand coverage.[5−8] Specifically, we shall represent the site energies as

$$\alpha_i = \alpha_0(1 + \delta\alpha_i) \equiv \alpha_0[1 + \delta\alpha(\text{ran}_i - 0.5)] \quad (2.2)$$

where ran_i is a random number between 0 and 1 and the sampling is such that the mean value of the energy is α_0, i.e., $\sum_{i=1}^{n} \Delta\alpha_i \equiv \alpha_0 \delta\alpha \sum_{i=1}^{n} (\text{ran}_i - 0.5) = 0$. We emphasize that the fluctuations in the site energies are chosen so as to average out to zero. The value of α_0 sets the zero of energy and so is not really needed, but the range, $\Delta\alpha_i \equiv \alpha_0 \delta\alpha$, of the fluctuation in the site energies is a critical parameter. It is determined by the width of the size distribution that, in the companion paper,[17] is quite narrow, and we use $\delta\alpha = 5\%$. Larger values are easier to achieve, and we emphasize that, for an expanded lattice, wider fluctuations in the site energies, if comparable to the Coulomb repulsion energy I, can lead to a qualitatively different behavior.[24] Since $\Delta\alpha_i \equiv \alpha_0 \delta\alpha$, this regime can also be reached by changing the value of α_0, i.e., by changing the composition of the dots.

The transfer integral β depends on the distance $D/2R$ between the dots, and we use the following functional form:

$$\beta = (\beta_0/2)(1 + \tanh[(D_0 - D)/4LR]) \quad (2.3)$$

which decays exponentially as $\beta_0 \exp(-D/2RL)$ at large inter-dot separation. Figure 2 shows a plot of (2.3) with the L parameter determined from a fit of the measured second harmonic optical response.[8] The decline is steep because $1/L = 5.5$. This implies a relatively swift change from weak to strong coupling when we vary $D/2R$, and this will be a key feature of our results. We therefore point out that this choice of $1/L$ is further discussed in refs 8 and 19. For future reference we note that we take the point of inflection $D_0/2R$ to equal 1.2 so that the inter-dot coupling falls to half its maximal value at $(D/2R) = 1.2$. It is this which will be shown to determine the boundary between the strong coupling (Anderson) regime and the weak coupling (Mott) regime. Figure 2 shows the range of fluctuations in the site energies (dashed area) so as to emphasize

(20) Paldus, J. *J. Chem. Phys.* **1974**, *61*, 5321−5330.
(21) Paldus, J. In *Unitary Group Approach to Many-Electron Correlation Problem*; Paldus, J., Ed.; Springer: Berlin, 1981; Vol. 22, pp 1−50.
(22) Remacle, F.; Levine, R. D. *J. Chem. Phys.* **1999**, *110*, 5089−5099.
(23) Hoffmann, R. *Solids and Surfaces: A Chemist's View of Bonding in Extended Structures*; VCH: New York, 1988.
(24) Remacle, F.; Levine, R. D. *Proc Natl. Acad. Sci. U.S.A.* **2000**, 97, 553−558.

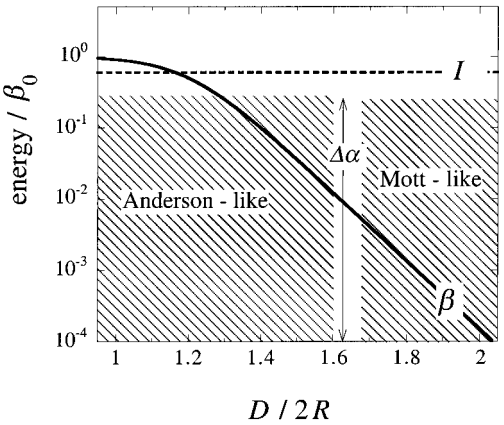

Figure 2. The three energies that determine the electronic structure of the array, plotted vs the lattice compression $D/2R$. See also Figure 1. I is the charging energy. For the narrow size distribution of the dots used in the experiment[17] that we discuss here, I is larger than the range, $\Delta\alpha$, of possible fluctuations in the energies of the dots. The actual energies, eq 2.2, fall within the shaded range. Two (not mutually exclusive) coupling regimes are indicated: In the Mott regime, the main effect is the role of the charging energy that tends to localize each electron on a dot (cf. Figure 1). In the Anderson regime, the dot−dot coupling is strong enough to overcome both I and the variations in the site energies.

that, at high compressions, the inter-dot coupling can exceed the variations in the site energies. β_0 is our unit of energy, and we scale all energies by it. Comparing with a physical system does, of course, require an explicit value.

The fluctuations in the dot−dot coupling β are governed by both the variation in the size, R, of the dots and the variation in the local packing distance D. This is unlike the case with the site energies, which vary only due to size variations. Hence, in general, β will fluctuate more than α.

The magnitude and range of the transfer integral β can be experimentally tuned in a number of ways, and this has not yet been fully explored. In particular, it may prove possible to alter the transfer integral β while keeping the composition of the dot, by changing the ligands. These can be involved as an active bridge for electron transfer. Increasing the range of the dot−dot coupling can markedly facilitate the onset of metallic behavior.

The last term in (2.1) is the Hubbard term. The two electron repulsion (Hubbard) terms in the Hamiltonian are often handled by a self-consistent field procedure. Instead, we will carry out a complete configuration interaction by using the unitary group formalism.[20,21,25] This is possible, since the Hamiltonian (2.1) is expressed in terms of the generators, $\hat{E}_{ij}$, of the unitary group $U(n)$, where n is the number of sites. These operators are spin independent and obey the commutation rules

$$[\hat{E}_{i,j},\hat{E}_{k,l}] = \hat{E}_{i,l}\delta_{j,k} - \hat{E}_{k,j}\delta_{i,l}, \quad i,j,k,l = 1, ..., n \qquad (2.4)$$

The diagonal generators $\hat{E}_{i,i}$ are called the weight generators, while the off-diagonal generators $\hat{E}_{i,j}$ are shift generators. Note that the Hubbard term in (2.1) involves diagonal generators only. Note that the Hubbard term ($\sum\hat{E}_{i,i}(\hat{E}_{i,i} - 1)$) simply counts the number of doubly occupied sites.

The computations require the value of the charging energy I. The charging energy can be estimated as

$$I = e^2/C(R) \qquad (2.5)$$

$C(R)$ is the size-dependent finite capacitance of an individual dot, $C(R) = 4\pi\epsilon_0\epsilon R$, where R is the radius of the dot, ϵ_0 is the permittivity of a vacuum, and ϵ is the dielectric constant of the material surrounding the particle. The experiments referred to below[6,16] were made for dots of $R = 35$ Å. Note that eq 2.5 determines also the local variations in I due to the variations in the size of the dots.

The Hamiltonian is diagonalized using its matrix representation in a basis of spin and symmetry-adapted many-electron zero-order states that belong to an irreducible representation of the group $U(n)$.[21] The details of the computations are given elsewhere.[22] Here we note that for an array, where a site has more than two near neighbors, implementing the commutation relations (2.4) in matrix form is carried out in a stepwise manner, starting from the generators for raising or lowering the site index by unity. The numbers of doublet states are $N = 784$, 2.821056160×10^9, and $5.934116446 \times 10^{19}$ for $n = 7$, 19, and 37, respectively. (The number, n, of sites is that of smallest hexagonal arrays.) The results we show below are for the seven-site array. The high degeneracy implied by the large number of electronic states means that care must be exercised in diagonalizing the Hamiltonian matrix. [The accuracy of numerical diagonalization methods is typically less for the eigenvectors than for the eigenvalues, and moreover, the eigenvectors of a subset of degenerate eigenvalues are defined up to a rotation that can be machine dependent. We got satisfactory results using the subroutine DSYEVD of the LAPACK library,[26] which also gives degenerate eigenvectors for which the rotation factor is not machine dependent. The accuracy of the results, and specifically the computation of the polarizability (which depends on matrix elements, see section 3), has been checked by computing on different machines.] This is particularly so at low compressions of the lattice where the coupling of the dots is weak.

2.1. The Zero-Order Description in the Weak Coupling Regime. The Hamiltonian for which the dots are uncoupled is quite simple:

$$H_0^1 = \alpha_0\sum_{i=1}^{n}\hat{E}_{ii} + \frac{I}{2}\sum_{i=1}^{n}\hat{E}_{ii}(\hat{E}_{ii} - 1) \qquad (2.6)$$

Without the Coulomb repulsion, all the doublet states of an n-site, n-electron (n odd) model are degenerate with an energy $n\alpha_0$. The Coulomb repulsion term counts the number of doubly excited site orbitals. For $n = 7$, the possible electronic configurations have zero, one, two, or three doubly occupied site orbitals with energies $7\alpha_0$, $7\alpha_0 + I$, $7\alpha_0 + 2I$, and $7\alpha_0 + 3I$, respectively. For an array of seven non-interacting dots, the Coulomb repulsion therefore leads to a splitting of the degenerate ground state into four bands of degenerate states. The ground state corresponds to electronic configurations with one electron per site and is unaffected by the Hubbard term. It is 14 times degenerate, and its energy is $7\alpha_0$. (There are 210 degenerate states at $7\alpha_0 + I$, 420 states at $7\alpha_0 + 2I$, and 140 states at $7\alpha_0 + 3I$).

When the fluctuations of the site energies (but not the charging energies) are taken into account, the energies of the zero states become

(25) Hinze, J. In *The Unitary Group for the Evaluation of Electronic Energy Matrix Elements*; Hinze, J., Ed.; Springer: Berlin, 1981; Vol. 22.

(26) Anderson, E.; Bai, Z.; Bischof, C.; Demmel, J.; Dongarra, J.; Croz, J. D.; Greenbaum, A.; Hammarling, S.; McKenney, A.; Ostrouchov, S.; Sorensen, D. *LAPACK Users' Guide*, Release 2.0; SIAM: 1994.

$$H_0^1 = \sum_{i=1}^{n} \alpha_i n_i + \frac{I}{2} n_i(n_i - 1) \tag{2.7}$$

where n_i is the number of electrons in the site i. The ground state has one electron per site and so is unaffected by the fluctuations in the site energies, beause they are sampled so as to average out to zero. Therefore, the ground state remains 14 times degenerate, and its energy is $n\alpha_0$. On the other hand, the energies of the three other bands are split by the fluctuations, and states from different bands can overlap if $\Delta\alpha > I$. Note that neither the charging energy I nor the range $\Delta\alpha$ of the fluctuations in the site energies is expected to vary strongly with the compression, particularly so in the regime of large inter-dot separation.

The near-neighbor coupling decreases exponentially with the inter-dot distance, cf. eq 2.3 and Figure 2, and at large separation is much smaller than I or the fluctuations $\Delta\alpha$. When the transfer coupling is included, the energies of the four bands of eigenstates of the Hamiltonian H_0^1 (including the band of the ground state) are split. The ground-state band is unaffected by the fluctuations in the site energies. When $I \neq 0$, there is a ground state band, and its splitting by the inter-dot coupling leads to the very small transition frequencies between the now nondegenerate ground state and very low-lying excited states. These very low frequencies, which decrease exponentially with increasing separation and are of the order of $\beta^2/I \approx 10^{-7}\beta_0$ for $D/2R = 2$, are seen in Figure 1. Note that they connect the ground state to delocalized excited states. The limit of $I \rightarrow 0$ is discussed in section 2.2.

To conclude, at larger values of $D/2R$ (when $D > D_0$, cf. eq 2.3), the Coulomb repulsion ensures that there can be a small (14 states for $n = 7$) band of lowest energy states. These are the states where each electron occupies a different site. When I exceeds the range, $\Delta\alpha$, of fluctuations in the site energies, this band is separated from other (770 for $n = 7$) states because only it has no Coulomb repulsion effects. This is the Mott regime. The inter-dot coupling splits this band and gives rise to very low-frequency transitions out of the ground state. If $I = 0$, there should still be 14 states whose energy is $7\alpha_0$, but they will lie in the middle of the band of 784 states, cf. Figure 1. It is the large Coulomb repulsion that sets the band of 14 states apart. On the other hand, when the range, $\Delta\alpha$, of fluctuations in the site energies exceeds I, the ground-state band of states will be mixed with the other (770 for $n = 7$) states, where there can be sites which are doubly occupied.

2.2. The Strong Coupling High-Compression Limit. We turn next to the opposite limit, that of high compression, where the dominant effect is the inter-dot coupling, β, which is larger than either $\Delta\alpha$ or I. A suitable zero-order ($I = 0$ and $\Delta\alpha = 0$) Hamiltonian is

$$H_0^2 = \alpha_0 \sum_{i=1}^{n} \hat{E}_{ii} + \beta \sum_{ij}^{n} \hat{E}_{ij} \tag{2.8}$$

This is the Hückel limit, and since $I = 0$, the one-electron level of description is valid. One can generate the many-electron states from the one-electron molecular orbitals (MOs) which are obtained by diagonalizing the $n \times n$ Hückel Hamiltonian matrix,

$$\mathbf{H}_{\text{Hückel}} = \alpha_0 \mathbf{I} + \beta \mathbf{M} \tag{2.9}$$

$\mathbf{M}$ is the adjacency matrix[27] whose nonzero entries $\mathbf{M}_{ij} = 1$ correspond to i and j being indices of adjacent sites. The eigenstates of the adjacency matrix determine the MOs which are fully delocalized and do not vary as the spacing is changing. The n eigenvalues of the Hamiltonian matrix (2.9) are the energies of the MOs and are given as $E_{\text{Hückel}} = \alpha_0 + \beta_m$, where m is one of the n eigenvalues of the adjacency matrix. Note that for $(D/2R) > 1$, m is independent of the compression so that the eigenvalues depend on $(D/2R)$ only through β, cf. eq 2.3. For an odd number of sites, the highest occupied MO in the ground state is degenerate. (It is doubly degenerate for our seven-site system, but the degeneracy can be higher for larger arrays.) This degeneracy is split by the fluctuations in the site energies $\Delta\alpha$. This splitting leads to a small transition frequency whose magnitude is therefore governed by $\Delta\alpha$.

2.3. The Intermediate Region: Coupled but Not Delocalized. Intermediate between the low-compression and high-compression regimes, there is a transition region where the distribution of frequency transitions is more uniform because β, I, and $\Delta\alpha$ are of the same order of magnitude so that there is no good zero-order Hamiltonian. In this region, there is no transition frequency that is more than an order of magnitude smaller than the next one. Outside of it there is a distinct lowest frequency transition, cf. Figure 1. But the origin and the magnitude of the smallest transition frequency are quite different in the low and in the high levels of compression of the lattice. On the right side of the intermediate region (low compression), the electronic states are localized on the sites. On the left side (high compression), the many-electron states are delocalized over all the sites of the lattice.

3. The Dielectric Response

This section provides the technical details for computing the contribution of the electronic states of the array to the dielectric function. The computation uses the exact expression as given by quantum mechanical linear response theory because the off-resonance terms give rise to a background contribution that is not negligible. The computations are quantum mechanical and do not include any thermally activated hopping contribution, which means that the very low-frequency limit need not agree with experiment. In terms of simple models, one can say that what we compute is a resonant and not a Debye-like[28,29] expression. The simplest representation of a resonant contribution is the VanVleck−Weisskopf[30] Fröhlich[28] functional form. However, here we use the quantum mechanical form of the polarizability and not a one-term approximation to it.

The starting form is the expression for the frequency-dependent electronic polarizability of a system. For the xx component,

$$\alpha_{xx}(\omega) = \frac{e^2}{\hbar} \sum_{m \neq g}^{N} |\langle g|x|m\rangle|^2 \times \left(\frac{1}{\omega_{mg} - i\Gamma_m - \omega} + \frac{1}{\omega_{mg} + i\Gamma_m - \omega} \right) \tag{3.1}$$

with obvious modifications for the other components. g is the ground state. The N electronic states are enumerated by m, $\omega_{mg} = \omega_m - \omega_g > 0$. Three factors govern the magnitude of

(27) Platt, J. R. In *Free Electron Theory of Conjugated Molecules*; Platt, J. R., Ed.; Wiley: New York, 1964.

(28) Fröhlich, H. *Theory of Dielectric: Dielectric Constant and Dielectric Loss*; Clarendon Press: Oxford, 1950.

(29) Kubo, R.; Toda, M. *Non Equlibrium Statistical Mechanics*; Springer-Verlag: Berlin, 1985.

(30) VanVleck, J. H.; Weisskopf, V. F. *Rev. Mod. Phys.* **1945**, *17*, 227−236.

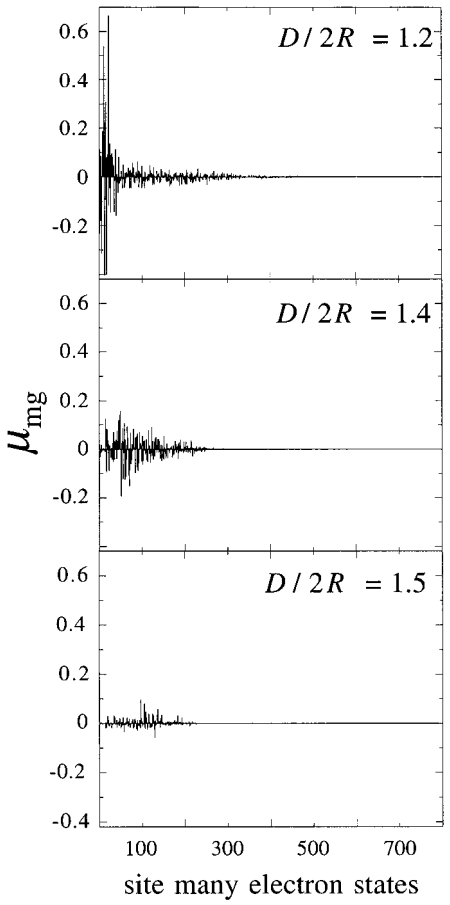

Figure 3. Dipole transition amplitude $\mu_{mg} = \langle g|x|m\rangle$ in the x direction, from the ground state to each excited state m, $m = 1, 2, ..., 783$. Shown for three values of the lattice compression, $D/2R$, as indicated. Had we plotted the transition strength, $|\mu_{mg}|^2$, itself, the small transitions would be hardly evident. There are two noteworthy aspects. One is the role of delocalization. A localized wave function on a hexagonal array without a packing disorder will have no dipole strength in the x direction. As the lattice is compressed, the dot−dot coupling, β, increases and the wave function is increasingly delocalized. The other point is the breaking of symmetry. For an ordered hexagonal array, where all dots are identical, there will be no allowed transitions in the x direction. When we allow disorder but put $I = 0$, there are only 24 allowed transitions. These are the 24 ways in which a single electron can be excited from an occupied to an unoccupied molecular orbital in a hexagonal array of seven sites. These are lower energy transitions. There are 783 excited states in all, and when $I \neq 0$, these are no longer pure Hückel states, so all transitions are allowed but many have very small strength.

the polarizability: the magnitude of the transition dipole, the transition frequency, and the damping width, Γ_m.

It is important to emphasize that only those excited states with allowed transitions from the ground state (i.e., $|\langle g|x|m\rangle|^2 \neq 0$) contribute to the sum (3.1). The dipole matrix elements were computed as in ref 19. Of the 783 excited states for a seven-site hexagonal array, there are only 24 allowed transitions at the Hückel level, but all transitions contribute when $I \neq 0$. Even so, the higher excited states tend to have the lower values of the transition dipoles because of their Hückel parentage: in the limit where $I = 0$, the high excited states have more than one electron occupying a higher molecular orbital. Such two (or more)-electron transitions are not allowed by a dipole transition. When I is finite, these states borrow some transition strength from the low excited states. The distribution of dipole strengths is shown in Figure 3. Note first that the overall magnitude clearly decreases as the lattice is expanded. This is why optical spectroscopy provides a good probe of the delocalization of the wave function. For an ordered hexagonal lattice there will be no dipole strength for a transition polarized in plane. Also, note how it is mostly the lower excited states that are optically accessible.

One can combine the two terms in (3.1),

$$\alpha_{xx}(\omega) = \frac{e^2}{\hbar}\sum_{m\neq g}^{N} \frac{2\omega_{mg}|\langle g|x|m\rangle|^2}{\omega_{mg}^2 + \Gamma_m^2 - \omega^2 - 2i\omega\Gamma_m} \tag{3.2}$$

so as to show the shift of the resonance frequency due to the damping. This quantum mechanical form, eq 3.2, of the polarizability agrees with the classical expression for the dielectric constant for the case of N damped harmonic oscillators representing, in the manner of Heisenberg, the transition modes of the electrons.[28,31]

Taking the real part and the imaginary parts of the polarizability shows the role of the damping:

$$Re[\alpha_{xx}(\omega)] = \frac{e^2}{\hbar}\sum_{m\neq g}\frac{2|\langle g|x|m\rangle|^2[(\omega_{mg}^2 + \Gamma_m^2) - \omega^2]}{[(\omega_{mg}^2 + \Gamma_m^2) - \omega^2]^2 + 4\omega^2\Gamma_m^2}$$
$$Im[\alpha_{xx}(\omega)] = \frac{e^2}{\hbar}\sum_{m\neq g}\frac{|\langle g|x|m\rangle|^2\omega_{mg}\Gamma_m}{[(\omega_{mg}^2 + \Gamma_m^2) - \omega^2]^2 + 4\omega^2\Gamma_m^2} \tag{3.3}$$

At $\omega = 0$, the contribution of the background to the electronic polarizability is real and positive:

$$\alpha_{xx}(0) = \frac{e^2}{\hbar}\sum_{m\neq g}\frac{2\omega_{mg}|\langle g|x|m\rangle|^2}{\omega_{mg}^2 + \Gamma_m^2} > 0 \tag{3.4}$$

As $\omega \rightarrow \infty$, $\alpha_{xx}(\omega) \rightarrow 0$ (both real and imaginary parts).

When ω goes through a resonance, $Re[\alpha_{xx}(\omega)]$ changes sign and goes from positive to negative while $Im[\alpha_{xx}(\omega)]$ goes through a maximum ($Im[\alpha_{xx}(\omega)]$ is positive for $\omega > 0$). The position of the resonance is governed by $\omega_{mg}^2 + \Gamma_m^2$ and so depends also on how the damping scales with the compression. We have used the functional form

$$\Gamma_m = C\omega_{mg}^3(1 + \beta_0/\beta) \tag{3.5}$$

where β, an exponentially decreasing function of $D/2R$, is given in (2.3) and C is an overall scale factor (Figure 2). This dependence is due to the competition between the damping on site and the transfer from one site to the next. The faster the transfer (h/β), the lower the damping rate. The result is that the damping has a part which decreases as $D/2R$ increases. The damping rate is an increasing function of the transition frequency ω_{mg} (higher excited states are more subject to damping).

The frequency-dependent dielectric constant is given by

$$\epsilon(\omega) = 1 + (N/\epsilon_0)\alpha_{xx}(\omega)$$
$$M(\omega) = 1/\epsilon^*(\omega) \tag{3.6}$$

where here N is the number of dots per unit volume and ϵ_0 is the vacuum permittivity, so that $(N(\epsilon_0)\alpha_{xx}(\omega)$ is dimensionless. The complex dielectric modulus is defined by $M = 1/\epsilon^*$ so that

(31) vonHippel, A. R. *Dielectric and Waves*; Wiley: New York, 1954.

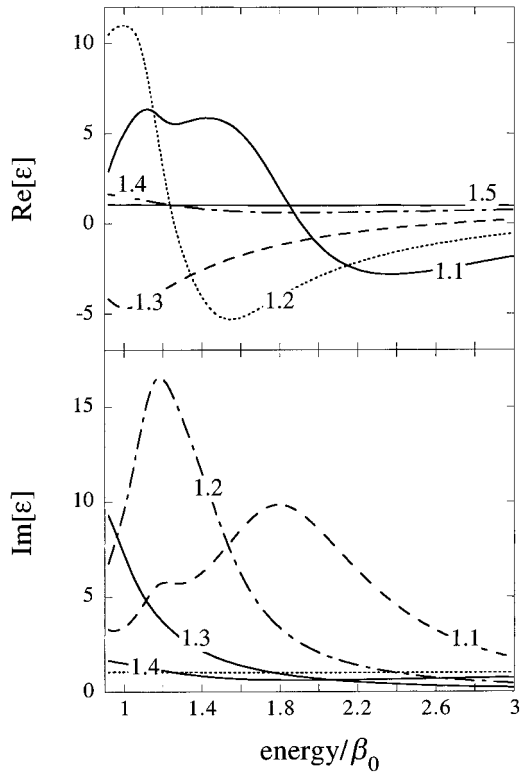

Figure 4. Real and imaginary parts of the dielectric constant, plotted vs the frequency for several values of the lattice compression, $D/2R$, as indicated. The energy axis is in units of β_0, eq 2.3, which determines the magnitude of the dot−dot coupling. The resonance we compute does shift as the lattice compression, $D/2R$, changes. The transition from an insulating to a metallic behavior occurs, as in the experiment[17] at $D/2R > 1.3$. This transition is very evident in a Cole−Cole plot (Figure 6). It is also worth noting that if we use the value, 0.5 eV, of β_0 that is obtained by a fit to the second harmonic response experiment,[8] then the resonance seen in the imaginary part occurs at the point which the present experiment[17] suggests is the energy of the collective resonance. To be sure that this is not an accident, it would be good to have a measurement of a third property. If confirmed, we will have at hand both the range and the magnitude of the dot−dot coupling.

$$M = 1/\epsilon^*(\omega) = \frac{\epsilon(\omega)}{|\epsilon(\omega)|^2} = \frac{\exp[i\phi(\omega)]}{|\epsilon(\omega)|}$$
$$\tan[\phi(\omega)] = \frac{Im[\epsilon(\omega)]}{Re[\epsilon(\omega)]} \qquad (3.7)$$

$Im[\epsilon(\omega)]$ is the dissipative part of the dielectric constant and is positive throughout the frequency range. $Re[\epsilon(\omega)]$ is the dispersive part. Through a resonance, $Re[\epsilon(\omega)]$ will become negative if $N/\epsilon_0 Re[\alpha_{xx}(\omega)]$ (eq 3.3) is smaller than -1. This will occur at high compression where the magnitude of β is large. Our results are that plotting M in a Cole−Cole plot (the real vs imaginary part as the frequency is varying) emphasizes the small $D/2R$ side of the metal insulator transition, while a Cole−Cole plot of ϵ itself is more sensitive to the larger $D/2R$ range. So, M is more sensitive to the role of the charging energy I, while the plot of the dielectric constant ϵ is more sensitive to the effect of the inter-dot coupling β. Operationally, this means that ϵ is more sensitive to the lower frequency range, while the plot of the dielectric modulus M is more sensitive to higher frequencies.

4. Results

The computations were carried out for a charging energy, $I = 0.6\ \beta_0$, and site energies $\alpha_0 = 10\ \beta_0$, $\delta\alpha = 0.05$ (dimensionless), due to size fluctuations. We also include a 5% fluctuation in packing.

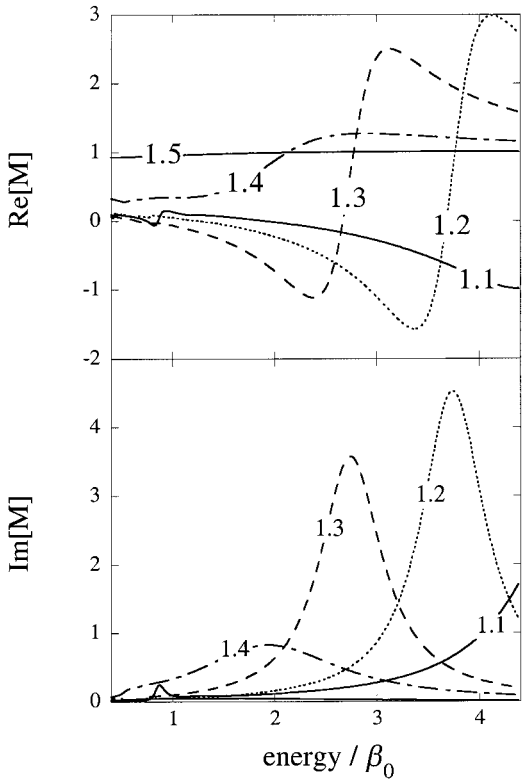

Figure 5. Real and imaginary parts of the dielectric modulus, M, plotted vs the frequency for several values of the lattice compression, $D/2R$, as indicated. The energy axis is in units of β_0, eq 2.3. Note that the energy axis extends to a higher range than in Figure 4. This is to show that the variation of M is more sensitive to the role of the charging energy while a plot of the dielectric constant is more sensitive indicator of the role of the dot−dot coupling.

The behavior of the dielectric constant $\epsilon(\omega)$ at very low (microwave range) frequencies and a comparison with these experimental results[6,16] is discussed in detail in notes available from us. We do not show these results here because, at the moment, it is not clear to us to what extent the low-frequency transport measurements are due to thermally activated charge migration.

The dielectric constant $\epsilon(\omega)$ has been measured at much higher frequencies via the optical transmittance and reflectance of the monolayer.[5,6,17] In this region, $\epsilon(\omega)$ exhibits a resonance behavior. Our computations also show a strong resonance in this frequency range. In Figure 4, the real (panel a) and imaginary (panel b) parts of $\epsilon(\omega)$ are plotted as functions of the frequency ω for several values of $D/2R$: from a high compression value to a lower compression. At low compression ($D/2R > 1.4$), $Re[\epsilon(\omega)]$ is positive and very small because we compute only the contribution of the array to the dielectric response. On the other hand, for higher compressions, $Re[\epsilon(\omega)]$ has clearly a dispersive character, and the resonance occurs at higher frequencies as $D/2R$ decreases. This behavior is similar to that observed experimentally. The imaginary part of $\epsilon(\omega)$ (panel b) is always positive and less sensitive to compression than the real part. This too is as observed. The resonance seen in panel b may be the resonance suggested in the experimental companion paper[17] to be in the near-IR. This interpretation is consistent with the value, 0.5 eV, of β_0 that we obtained[8] by fitting the measured nonlinear optical response as a function of lattice compression.[7]

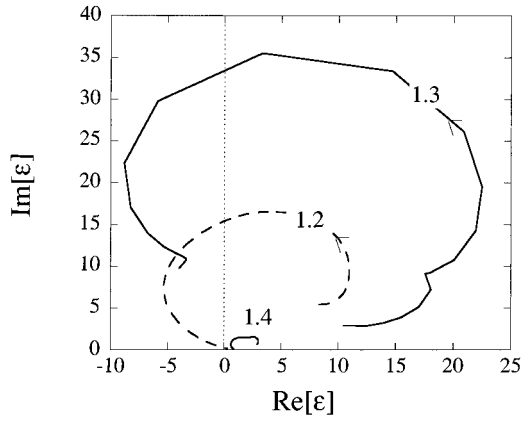

Figure 6. Cole−Cole plot of the imaginary vs the real part of the dielectric constant as the frequency is varied. Increasing the frequency makes the plot change in an anticlockwise fashion. The key point to compare with experiment is that for an insulating array, the dielectric constant plot is confined to the positive quadrant. It is also much smaller, cf. Figure 8 of ref 17.

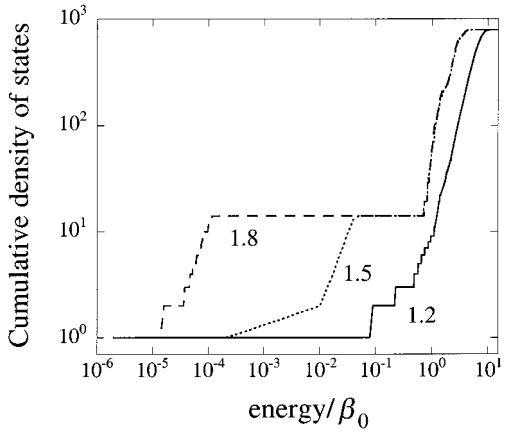

Figure 7. The number of quantum states which are below a given energy plotted as a function of the energy. At low compressions there is a band of very low lying states followed by a gap, as can also be seen in Figure 1. At higher compression the number of states remains unity (viz., the ground state) until a higher energy, at which point it rises in a nearly continuous fashion. The first step at higher compression is due to the isolated low-lying excited state (cf. Figure 1). The next few steps are due to states that are hardly resolved on the scale of Figure 1.

Figure 5 compares the frequency dependence of $\epsilon(\omega)$ with that of $M(\omega)$. Note that the frequency scales in Figures 4 and 5 are different. This is because $M(\omega)$ is more sensitive to the high-frequency range of the spectrum. This is the range where the role of I is more important because it induces the intensity borrowing that is needed. In contrast, $\epsilon(\omega)$ is more sensitive to the lower frequency range, where it is the delocalization of the wave function that is most important.

Figure 6 shows a Cole−Cole plot of the dielectric constant for several lattice spacings. At high compression, when the dot−dot coupling is large and the wave function is delocalized, the plot is a counterclockwise circle centered so that fairly large negative values of $Re[\epsilon(\omega)]$ are possible. In the insulating phase, $\epsilon(\omega)$ stays in the positive quadrant. It is also much smaller because the dipole strength is greatly reduced (see Figure 3).

Finally, Figure 7 shows the number of states (i.e., the cumulative density of states which is how many states there are up to a given energy) vs energy at three levels of compression, $D/2R = 1.2$, 1.5, and 1.8. While the density of states is almost continuous for $D/2R < 1.4$, at lower levels of compression it exhibits a wide gap that corresponds to the charging energy I, in agreement with the experimental results.[13] The origin of the gap at wider spacings is, as discussed in Figure 1, namely the splitting off of the ground-state covalent band due to the exponentially small coupling to the ionic states. It is the closing of this gap upon compression that marks the onset of facile charge exchange between adjacent dots. As emphasized in section 2.3, this is not necessarily the same as the onset of extensive delocalization.

5. Summary

The electronic contribution to the dielectric response as a function of frequency can be computed from the quantum mechanical electronic polarizability of the lattice. The polarizability is the sum of the oscillator strengths, each weighted by a resonance denominator. There are many possible final states (cf. Figure 1), but the width of the resonance smoothes the electronic response as a function of frequency, giving rise to one broad peak. The larger amplitude of this peak when the lattice is compressed, as seen in the experiment, is here due to the better overlap of the wave functions of adjacent dots. (This gives rise to a larger transition dipole.) The energy of the states shifts as a function of the lattice compression, as shown in Figure 1. The computations were made for a hexagonal array of seven quantum dots, by a full diagonalization of the Hamiltonian in a many-electron basis, for different values of the distance between the dots. Particular attention was given to the role of small variations in the size, shape, and environment of the dots and to the Coulomb blocking due to the charging energy of the dots. When the dots are far apart, the electronic response is dominated by the Coulombic repulsion of electrons on a given dot. This gives rise to a Mott-like insulator−metal transition as the extended array is compressed. The transition is sensitive to the size of the dots. Upon further compression, the electronic response is dominated by the coupling between the dots. Comparison was made with experimental results for the dielectric response (preceding paper), and the qualitative agreement is encouraging.

Acknowledgment. We thank Gil Markovich, Pat Collier, and James Heath for many useful discussions and insights. We thank Oded Agam for critical discussions about the decoherence of the electrons. We had the benefit of correspondence with Joseph Paldus and Reuben Pauncz about the unitary group basis. SFB 377 and the Alexander von Humboldt Foundation supported this work. R.D.L. acknowledges support by the James Franck Program. F.R. thanks Action Recherche Concertée, Liège University, Belgium.

JA9915448